

Self-Complexation of Poly(ethylene oxide)-*block*-poly(methacrylic acid) Studied by Fluorescence Spectroscopy

Susanna Holappa,[†] Lauri Kantonen,[†] Françoise M. Winnik,[‡] and Heikki Tenhu^{*,†}

Laboratory of Polymer Chemistry, Department of Chemistry, University of Helsinki, PB 55, FIN-00014 University of Helsinki, Finland, and Faculty of Pharmacy and Department of Chemistry, University of Montreal, C.P. 6128 succ. Centre-Ville, Montreal, Quebec, Canada H3C 3J7

Received April 30, 2004; Revised Manuscript Received June 28, 2004

ABSTRACT: The evolution of the self-complexation of poly(ethylene oxide)-*block*-poly(methacrylic acid), PEO-*block*-PMAA, as a function of the degree of ionization has been studied by means of fluorescence spectroscopy and dynamic light scattering. Pyrene and naphthalene singly labeled block copolymers were used, with two different methacrylic acid block lengths. The conformation of the block copolymers changes with varying degree of ionization due to the hydrophobic nature of the methyl group of the methacrylic acid units as well as due to the hydrogen bonding that takes place between the methacrylic acid units and ethylene oxide units. The limiting degrees of ionization between the states where the block copolymers are molecularly dissolved or intra- or intermolecularly complexed were determined. The chain exchange between the self-complex particles at low degree of ionization was observed to take place via two mechanisms. Insertion and expulsion of the single chains is responsible of the faster exchange event whereas the slower chain exchange occurs by merging and splitting of the self-complex particles.

Introduction

The importance of noncovalent interactions in guiding the assembly of natural and synthetic systems has been long recognized, and more recently, strategies based on weak interactions have been devised to create functional nanosystems. The weak forces at play belong to three categories: electrostatic forces, hydrogen bonds, and the so-called hydrophobic interactions.¹ Very often they act in concert, and it is difficult to ascertain the true mechanism of the interactions and to assess the relative contribution of each force. Of interest here are objects formed via hydrogen bonds between hydrogen donors, such as nondissociated polyacids, and hydrogen acceptors, such as poly(ethylene oxide) (PEO)^{2–4} or polyethoxylated nonionic surfactants.⁵ Complexation occurs readily between PEO and protonated polyacids, but ionization of the polyacids at high pH reduces or even prevents their ability to form hydrogen bonds. The association in water of poly(ethylene oxide) (PEO) and either poly(methacrylic acid) (PMAA) or poly(acrylic acid) (PAA) has been studied by a variety of techniques, such as viscometry,^{6,7} sedimentation,⁸ potentiometric titration,^{6,7,9–12} fluorescence spectroscopy,^{2,11–13} NMR spectroscopy,¹⁴ and small-angle neutron scattering (SANS).⁴ In water of acidic pH, complexes of PMAA and PEO form, with 1:1 repeating molar units, as long as the molecular weight of PEO exceeds a threshold value of ~2000.^{9,10} The complexes are broken by neutralization of PMAA or by addition of alcohols, which disrupt the hydrogen bonds and modify the hydrophobicity of the complexes.^{15,16} As hydrophobic stabilization accounts, in part, for the complexation, an increase in solution temperature tends to enhance the stability of the complexes.

Hydrogen bonds can form also between PEO and PMAA or PAA fragments linked covalently, as in poly(methacrylic acid)-*block*-poly(ethylene oxide) (PMAA-*block*-PEO)^{17–19} or (PMAA-*graft*-PEO),²⁰ where a few PEO chains are linked covalently to a PMAA backbone. In acidic aqueous solutions of these copolymers, complexation can occur either among PMAA and PEO blocks of two different polymer chains, triggering the formation of polymeric micelles or between the blocks of a single macromolecule leading to “self-complexation”. The interplay between self-complexation and interpolymeric association offers the opportunity to modulate the solution properties of PMAA-*block*-PEO via subtle changes in solution temperature or pH. Gohy et al.¹⁷ have reported the solution properties of PMAA-*block*-PEO copolymers, consisting of long PEO blocks (177 and 200 EO units) and short PMAA blocks (21 and 41 MAA units, respectively). In acidic aqueous solution, the highly asymmetric block copolymers form micelles that exhibit marked temperature dependence. They form only in the 15–50 °C temperature range. Their stability is maximal when the solution temperature is 40 °C. Rearrangement occurs upon further heating, leading to macroscopic phase separation in the 40–55 °C temperature range, which encompasses the cloud point (50 °C) of PMAA. Note that under the conditions employed in this study the PEO/PMAA complexation involves both intra- and interchain hydrogen bonds and leaves a large number of EO units uncomplexed.

We reported recently the preparation of asymmetric PMAA-*block*-PEO copolymers,^{18,19} possessing a short EO block (ca. 113 EO units) and a MAA block of 207 units¹⁸ or either 122 or 294 units,¹⁹ which were shown to form interpolyelectrolyte complexes with various polycations.^{19,21} By contrast to Gohy et al.’s research, the MAA block is longer than the EO block. However, as long as the MAA block is sufficiently long in comparison to the EO block, stable micelles with narrow size distributions were formed at low pH as was shown

[†] University of Helsinki.

[‡] University of Montreal.

* Corresponding author: Tel +358-9-191 50334; Fax +358-9-191 50330; e-mail heikki.tenhu@helsinki.fi.

by dynamic light scattering measurements.^{18,19} The self-complex particles stabilized by the excess MAA units showed a similar temperature dependence¹⁸ as those where the EO units were in excess.¹⁷

We address here issues related to the complexation of the EO and MAA blocks of the copolymers, either within the same copolymer or between blocks of two different polymers. As the number of EO units in each copolymer is lower than the number of MAA units, complexation leaves MAA units uncomplexed, and consequently, the solutions properties of the block copolymers complexes are expected to reflect, to some extent, features intrinsic of the PMAA chains, particularly in the case of the larger block copolymer. It has been known for a long time that, unlike PAA chains which expand smoothly with increasing charge of the polymer, PMAA chains resist expansion before a critical charge density is attained.^{22,23} This dependence of the apparent ionization constant on the degree of ionization has been taken as an indication of a cooperative transition between two chain conformations and to reflect the occurrence, in the nonionized form of PMAA, of long-range attractive interactions between the hydrophobic methyl substituents which provide a powerful resistance to chain expansion, until a large fraction of the carboxylic groups are ionized.

We describe here a study of PEO-*block*-PMAA copolymers in water by two complementary techniques: dynamic light scattering (DLS) and fluorescence spectroscopy. While DLS provides a view of the polymeric micelles on the 2–100 nm distance scale, fluorescence spectroscopy affords a look at the molecular interactions within a single macromolecule or between different chains. We have prepared fluorescently labeled derivatives of PEO-*block*-PMAA (1 and 2), keeping the fluorescent tag content of the polymers low, in order not to affect significantly the solution properties of the copolymers. The labels, pyrene (Py) or naphthalene (Np), were linked to carboxylic acid residues of the PMAA blocks via polymer-analogous amidation.²⁴ The two chromophores were selected as they are capable of undergoing nonradiative energy transfer and, consequently, report on the proximity of two chains labeled, one with Py and the other with Np. Moreover, Py photophysics convey information on the polarity of the probe environment via changes in the relative intensity of characteristic bands of the emission spectrum and in fluorescence lifetime. The objectives of the study were to monitor the photophysical properties of the copolymers in solution, examining specifically the influence of the ionization degree of the copolymers on the properties of their solutions at room temperature. Particular attention was paid to the effect of the MAA block length on the hydrogen-bonded inter- and intrapolymeric complexation of the PEO-*block*-PMAA and to the kinetics of the exchange of chains among polymeric micelles.

Experimental Section

Materials. 1-Pyrenemethylamine hydrochloride (95%, Aldrich), 1-(1-naphthyl)ethylamine (98%, Aldrich), and 1,3-dicyclohexylcarbodiimide (DCC, Fluka) were used as received. Triethylamine (Merck) was distilled from NaOH under nitrogen before use. DMF was dried over CaH₂ overnight, distilled under reduced pressure, and stored under N₂ prior to use. Deionized water was obtained from a Milli-Q water purification system.

Preparation of the Labeled Polymers. Naphthalene- and pyrene-labeled block copolymers were prepared by labeling

Table 1. Properties of the Labeled Block Copolymers

	pyrene content		naphthalene content	
	mol % of MANa units	10 ⁻⁵ mol/g	mol % of MANa units	10 ⁻⁵ mol/g
Py-PEO- <i>block</i> -PMANa1 ^a	0.36	2.632		
Py-PEO- <i>block</i> -PMANa2 ^b	0.25	2.045		
Np-PEO- <i>block</i> -PMANa1 ^a			1.61	11.96
Np-PEO- <i>block</i> -PMANa2 ^b			1.68	13.38

^a PEO-*block*-PMANa1:¹⁹ $M_w = 22\,800$ g/mol, $M_n = 15\,800$ g/mol, $X_{n,MANa} = 122$. ^b PEO-*block*-PMANa2:¹⁹ $M_w = 74\,800$ g/mol, $M_n = 47\,100$ g/mol, $X_{n,MANa} = 294$. M_n of PEO block 5000 g/mol, $X_{n,EO} = 113$.

two copolymers PEO-*block*-PMAA1 and PEO-*block*-PMAA2 that differ by the size of the PMAA block. They were obtained, as described previously,¹⁹ via a two-step procedure involving, first, free radical polymerization of MAA and, second, attachment of α -amino- ω -methoxy-PEG ($M_n = 5000$) to the end of the PMAA chain. The copolymers were isolated in the sodium salt form by freeze-drying from aqueous solutions. The molecular weights of PEO-*block*-PMANa1 and PEO-*block*-PMANa2, determined by SEC, are $M_w = 22\,800$ g/mol ($M_w/M_n = 1.44$) and $M_w = 74\,800$ g/mol ($M_w/M_n = 1.59$), respectively. The two copolymers were labeled by following the procedure described by Anghel et al.²⁴ for the modification of poly(acrylic acid). 1-Pyrenemethylamine hydrochloride (1 mol % of MAA units) or 1-(1-naphthyl)ethylamine (2.5 mol % of MAA units) in DMF was added to a solution of the copolymer in DMF (2 wt %) kept at 60 °C under N₂. Next, TEA (1.1 times the molar amount of the label) and DCC (1.1 times the molar amount of the label) were injected into the reaction mixture. The reaction was let to proceed in the dark for 24 h. The reaction mixture was then cooled to room temperature and subjected to dialysis (CelluSep T2 regenerated cellulose membrane, MWCO 6000–8000) against DMF:H₂O mixtures of decreasing DMF content. The dialysis was continued until a label-free dialysate was obtained, as assessed from its UV absorbance and fluorescence spectra. The labeled copolymers were isolated by freeze-drying in their sodium salt form. The degree of labeling of each sample (Table 1) was determined from the UV absorbance of the labeled block copolymers dissolved in MeOH/H₂O 1/3 v/v (naphthalene-labeled polymer) or in water (pyrene-labeled polymers), using 1-(1-naphthyl)ethylamine and 1-pyrenemethylamine hydrochloride as model compounds ($\epsilon_{Py,341\text{ nm}} = 40\,127$ L mol⁻¹ cm⁻¹ and $\epsilon_{Np,280\text{ nm}} = 6607$ L mol⁻¹ cm⁻¹).

Methods. ¹H NMR spectra were recorded either on a Varian Gemini 2000 or on a Bruker Avance-400 spectrometer, using polymer solutions in D₂O. UV absorbance spectra were measured with either a Shimadzu UV-1601PC UV-vis spectrophotometer or a Hewlett-Packard 8452A diode-array spectrometer.

Potentiometric Titrations and pH Measurements. The potentiometric titrations of the block copolymers were performed by using a PHM210 standard pH meter (Meterlab, Radiometer, Copenhagen) calibrated with pH buffer standards 4.0 and 10.0 (Merck) prior to each titration. The polymer solutions of 0.5 g/L in 0.05 M aqueous NaOH were titrated with 0.1 M aqueous HCl. The titrations were performed from pH 12 to pH 2, allowing a 3 min equilibrium time for each point.

The pH of block copolymer sample solutions was measured after 12 h upon addition of HCl to copolymer solutions by using a PHM210 standard pH meter (Meterlab, Radiometer, Copenhagen) calibrated with pH buffer standards 4.0 and 10.0 (Merck). All pH measurements were done at 25 °C.

Fluorescence Measurements. Steady-state fluorescence spectra were recorded on a Fluorolog Tau-3 spectrometer (Jobin-Yvon Horiba) equipped with a GRAMS/32 (Galactic Ind) data analysis system. Temperature control of the samples was achieved using a water-jacketed cell holder connected to a Neslab circulating bath. All measurements were carried out

at 25 °C, unless otherwise stated. The slits were set at 0.5–0.6 mm (excitation) and 0.2–0.3 mm (emission) depending on the chromophore concentration. Emission spectra were obtained with excitation wavelengths of 342 nm (pyrene-labeled polymers) and 290 nm (naphthalene-labeled polymers). Excitation spectra were measured in the ratio mode and were monitored at 380 nm. Fluorescence lifetime measurements were conducted on a Fluorolog Tau-3 multifrequency phase modulation fluorimeter (Jobin-Yvon Horiba). The excitation light from a 450 W xenon lamp was modulated with a Pockels cell. Phase and modulation values were determined relative to a glycogen aqueous solution. The excitation wavelength was set at 342 nm. The pyrene emission was monitored at 376 nm. The frequency of the analyzing light was chosen in the range 0.1–100 MHz. All measurements were carried out at 25 °C, unless otherwise stated. Data were analyzed with the Data-max Spectroscopy software based on GRAMS/32 from Galactic Ind. Data were fit to a multiexponential decay law, $F(t) = \sum_i a_i e^{-t/\tau_i}$, where a_i and τ_i are the preexponential factors and the lifetime of the i th component, respectively. The goodness of the fit was determined by the χ^2 value and examination of the residuals. The preexponential factors a_i are related to the observed fractional intensity contribution f_i by the relation $f_i = a_i \tau_i / \sum_i a_i \tau_i$. The average lifetime $\langle \tau \rangle$ was calculated from $\langle \tau \rangle = \sum_i f_i \tau_i$.

Dynamic Light Scattering (DLS). DLS measurements were performed with a Brookhaven Instruments BI-200SM goniometer connected to a BI-9000AT digital correlator and equipped with an Ar laser ($\lambda = 514.5$ nm) and at an angle of 90°. The data were analyzed by the CONTIN algorithm. The temperature of the sample cell was controlled by LAUDA RC6 CP (water/glycol 1:1 circulation bath) thermostat.

Solutions for Analysis. In all cases, the samples were prepared from the sodium salt forms of the block copolymers, and polymer solutions of suitable concentration were prepared by dilution of a polymer stock solution (1.0 g/L). After dilution, the solutions were kept at room temperature for 12 h prior to measurements. For fluorescence measurements, the polymer concentrations of 0.1 g/L in aqueous NaCl (10 mM) were applied. The solutions were not degassed. In the case of the experiments based on NRET, mixed solutions were prepared as follows: Method 1: predissolved Py-PEO-*block*-PMANa and Np-PEO-*block*-PMANa. The aqueous 1 g/L stock solutions consisting of either Py-labeled or Np-labeled block copolymers were mixed and were allowed to stabilize for 30 min. Subsequently, desired dilutions were made with water, the ionic strength was adjusted with 20 mM NaCl solution, and the pH of the solutions was fixed with 0.1 M HCl. Method 2: codissolution of Py-PEO-*block*-PMANa and Np-PEO-*block*-PMANa. The Py- or Np-labeled block copolymers were mixed as dry polymers and then dissolved in water to obtain 1 g/L stock solution, which was allowed to stabilize for 12 h. The following steps in sample preparation were as above. In both methods and for both block copolymers, PEO-*block*-PMAA1 and PEO-*block*-PMAA2, the molar ratio [Np]:[Py] was adjusted to 4:1. For DLS measurements, the aqueous block copolymer stock solutions were diluted with 50 mM NaCl to obtain a polymer concentration of 0.5 g/L and an ionic strength of 25 mM. The pH of all solutions was set to the desired value by dropwise addition of aqueous HCl (0.1 M).

Data Analysis. *Potentiometric Titration.* The dissociation equilibrium of a weak polyacid can be quantified by determining the apparent dissociation constant K_a via equation

$$pK_a = \text{pH} + \log\left(\frac{1 - \alpha}{\alpha}\right) \quad (1)$$

The experimental pH values and the degrees of dissociation α are obtained from the potentiometric titrations. The degrees of dissociation, $\alpha = 1$ and $\alpha = 0$, were determined from the inflection points of the titration curve by using a second-derivative method.

DLS Analysis. The time correlation functions were analyzed with a Laplace inversion program CONTIN. The polydispersity

index (PDI) of the particles was determined from the μ_2/T^2 ratio from the cumulant fit of the second order.

Analysis of the Steady-State Fluorescence Spectral Data. The ratio I_1/I_3 was obtained from the intensity of the pyrene emission at 375 nm (I_1) and at 386 nm (I_3). The ratio I_{Py}/I_{Np} was calculated from the average intensity of the emissions at 323 nm and at 338 nm (I_{Np}) and at 396 nm (I_{Py}). To analyze the nonradiative energy transfer kinetic data, the naphthalene emission intensity at a given time t (I_t) was plotted as a function of the time and fitted to eq 2:

$$I_t = I_0 - f_1(1 - e^{-k_1 t}) - f_2(1 - e^{-k_2 t}) \quad (2)$$

where I_0 is the initial Np emission intensity (set to 1), f_1 and f_2 are the fractions of the fast and slow chain exchange events, and k_1 and k_2 are the kinetic coefficients for the fast and slow events, respectively.

Results

Synthesis and Characterization of the Labeled Block Copolymers. Attachment of the labels to the PMAA blocks was achieved by reaction of carboxylic acid residues with chromophores carrying a primary amine linked to a short alkyl chain. The reactions were performed in an aprotic solvent, dimethylformamide, in the presence of 1,3-dicyclohexylcarbodiimide (DCC) and triethylamine. Under these conditions, random attachment of the hydrophobic groups along the macromolecule is favored over the formation of discrete blocks of contiguous chromophores.²⁵ Specifically, the copolymers were labeled with pyrene by reaction with 1-pyrenylmethylamine and with naphthalene (Np) by reaction with 1-naphthylmethylamine. The purified copolymers were isolated in the sodium salt form. In all, four polymer samples were prepared. The polymers were characterized by UV absorption spectroscopy for calculation of the level of labeling (Table 1).

Potentiometric Titration. The ionization energy of a polyelectrolyte increases with increasing degree of ionization. Therefore, the dissociation constant pK_a of a polyelectrolyte is not constant throughout the degree of ionization range. Also, the conformational transitions of the polyelectrolytes cause nonlinearity into the pK_a vs α curves. PMAA is one of the polyelectrolytes that belong to this group due to the α -methyl group. On the basis of the early studies of Nagasawa et al.²⁶ and Leyte et al.,²⁷ the nonlinearity of pK_a vs α is strongly dependent on the tacticity of the polymer and the ionic strength of the solution. The proximity of the carboxylic acid groups depends on the tacticity of PMAA. Therefore, at low α , when the polymer is contracted, more electrostatic work is required to remove H^+ from isotactic PMAA in comparison to syndio- and atactic polymers. As a result, $pK_{a,iso-}$ increases faster than the other pK_a s. When a certain fraction of the acid groups are ionized, the osmotic pressure exceeds the contracting force of the hydrophobic interactions between the α -methyl groups. A remarkable expansion of the coil takes place, which prohibits the increase of the charge density. This is seen as a plateau or even as a negative slope in the pK_a curve. Once the extended conformation is reached, further ionization turns again more difficult, and as a result the pK_a increases again.

Increasing ionic strength decreases the value of pK_a , shifts the plateau region to higher α , and turns the slopes of the different parts of the pK_a vs α curve less steep. This is because the alterations in the pK_a are affected by repulsion between the charges along the polymer chain.²⁷

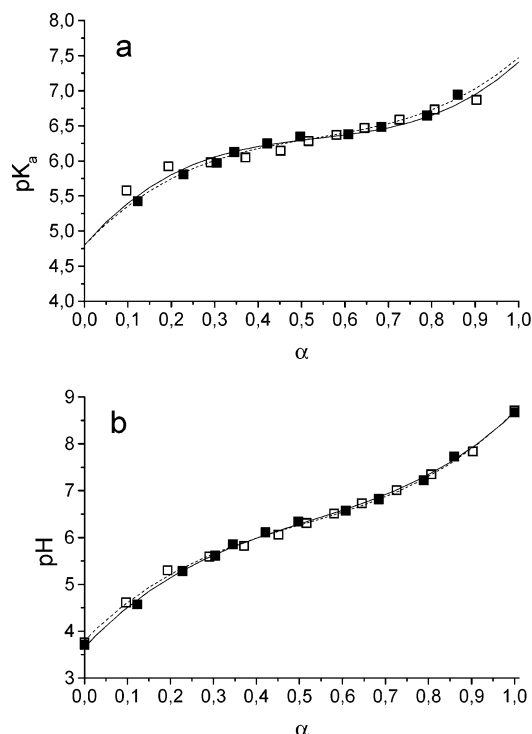


Figure 1. (a) pK_a and (b) pH of PEO-*block*-PMAA1 (solid symbol) and PEO-*block*-PMAA2 (open symbol) against α . Polymer solutions of concentration 0.5 g/L in 50 mM NaOH were titrated with 100 mM HCl.

Parts a and b of Figure 1 present the apparent pK_a values of the block copolymers and the pH of the solutions against α , respectively. The shapes of the pK_a and pH curves coincide with those typical for syndio- and atactic PMAA at ionic strength of $c_{\text{MAA}} < c_{\text{NaCl}}$.^{26,27} The pK_a increases up to $\alpha = 0.3$; there is a plateau-like region at $0.35 < \alpha < 0.6$, after which the slope increases again. In the study of Wang et al.,²⁸ aggregation behaviors of random and block copolymers of MAA and ethyl acrylate, EA, were compared. The shape of the PMAA-*block*-PEA pK_a curve coincides with the titration curves of the present study, whereas the changes of the pK_a of the random copolymer are more remarkable. The difference in the potentiometric behavior is seen to rise from the difference in the particle morphology at low pH. The random copolymer forms random latex particles in which some of the carboxylic groups are trapped inside the compact latex particles. At low pH, the ionization of the acid groups is energetically very unfavorable due to the closeness of the other acid groups. Therefore, the pK_a undergoes a sudden increase. At certain point the particles begin to disintegrate with increasing α , which makes the extending of the polymers possible. Consequently, the dissociation of the protons from the polyacids is more favorable, thus inducing decreasing pK_a . The particles formed by the block copolymer have a micellar morphology, hydrophobic EA core, and a corona composed of MAA. The ionization of the MAA groups is easier in the particle shell in comparison to the ionization in the random aggregates, and a potentiometric curve similar to Figure 1 is obtained. Therefore, it is reasonable to consider the PEO-*block*-PMAA particles more as micellar than as randomly aggregated particles.

Dynamic Light Scattering. We have explored several experimental approaches to detect the formation of polymeric micelles via complexation of PEO-*block*-

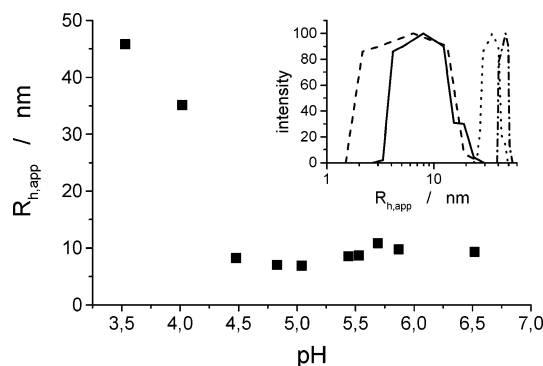


Figure 2. Apparent hydrodynamic radius, $R_{h,\text{app}}$, of PEO-*block*-PMAA2 as a function of solution pH. Inset: size distributions at pH 3.5 (dash-dotted line), pH 4.0 (dotted line), pH 4.5 (dashed line), and pH 6.5 (solid line); polymer concentration = 0.5 g/L, $I = 25$ mM.

PMAA and their disruption in response to an external stimulus,^{19,21} but by far the most direct technique is dynamic light scattering, which detects the presence of polymeric micelles and readily provides their apparent hydrodynamic radii (R_h). DLS measurements confirmed the presence of polymeric micelles in solutions of the fully protonated PEO-*block*-PMAAs, with an apparent R_h value of 45 nm in the case of the largest copolymer (PEO-*block*-PMAA2). Increasing the pH of the solution triggered several events: First, a sharp decrease of the size of the scattering object, which reaches a minimum value of ~ 8 nm in the pH range $4.5 < \text{pH} < 5.5$, followed by a slight increase in R_h for pH above 5.5 (Figure 1). We envisage the following scenario to account for the trends observed by DLS. At low pH, when the copolymers are fully protonated, the carboxylic acid groups undergo hydrogen bonding with all the EO units available: interpolymeric micelles with a narrow size distribution form, consisting of a hydrophobic core of complexed PMAA and PEO (phase I, $\text{pH} < 4.5$, $\alpha < 0.07$). Upon further ionization of the carboxylic units, fewer hydrogen bonds can form with the EO units; the interpolymeric complexes are destroyed progressively, leading to free, but contracted, copolymer chains where complexation still occurs between EO units of one block and MAA units of the other (phase II, $4.5 < \text{pH} < 5.5$, $0.07 < \alpha < 0.3$). The intramolecular H-bonding is seen from the broadening of the size distribution to smaller sizes in comparison to the size distribution presenting the situation in phases III and IV (inset in Figure 2.). Intrapolymeric H-bonds are broken upon further ionization of the carboxylic groups, and the polymer chains take an uncomplexed conformation (phase III, $5.5 < \text{pH} < 6.0$, $0.3 < \alpha < 0.42$). However, only at $\text{pH} > 6$ (phase IV, $\alpha > 0.42$) the copolymer adopts the fully extended conformation characteristic of polyelectrolytes in water. We attribute the last chain expansion to the cooperative release of the hydrophobic interactions between the methyl groups of the PMAA block, a phenomenon related to the resistance to full extension in solutions of high pH exhibited by PMAA itself.

The inset of Figure 2 shows the representative size distributions of the PEO-*block*-PMAA at different pHs. In each case the distributions are monomodal, but the requirement of monodispersity, $\mu_2/\Gamma^2 < 0.1$, is fulfilled only at $\text{pH} < 4.5$. However, in each case the distributions present the self-diffusion of the polymer coils or complex particles, since the possibility of the

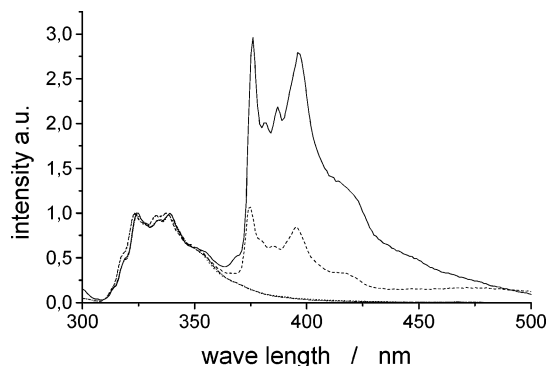


Figure 3. Fluorescence spectra of a mixed solution of Py-PEO-*block*-PMAA1 and Np-PEO-*block*-PMAA1 in aqueous solutions at pH 3.7 (solid line) and at pH 6.7 (dashed line) and of Np-PEO-*block*-PMAA1 at pH 3.7 (dash-dotted line) and at pH 6.5 (dotted line). The mixed solutions were obtained by codissolution of dry polymer samples; the total polymer concentration = 0.1 g/L, $I = 10$ mM, $[Np]/[Py] = 4$, $\lambda_{exc} = 290$ nm.

disturbing polyelectrolyte effect was excluded by using low ionic strength solution as a solvent so that $c_{NaCl} > c_{MAA}$.

This description of the interactions among and within the PEO-*block*-PMAA chains developed from DLS data was placed onto firmer ground by the analysis, described in the following sections, of the photophysics of labeled copolymers of varying degrees of ionization.

Fluorescence Spectroscopy. Nonradiative Energy Transfer Experiments. From the DLS measurements, we concluded that interpolymeric micelles form in acidic solutions of PEO-*block*-PMAA ($\alpha = 0$). To confirm this point, and to monitor the progressive disruption of the micelles upon increase of the degree of ionization of the copolymers, we conducted a series of spectroscopic measurements based on the nonradiative energy transfer (NRET) between naphthyl and pyrenyl groups linked to the PMAA blocks of different copolymers. The NRET process originates in dipole-dipole interactions between an energy donor in its excited state and an energy acceptor in its ground state.^{23,30} The probability of energy transfer between two chromophores depends sensitively on their separation distance and to a lesser extent on their relative orientation. Naphthalene and pyrene are known to interact as energy donor (Np) and energy acceptor (Py) in a nonradiative energy transfer process with a characteristic distance, R_0 , of 29 Å.³¹ In solutions where the Np- and Py-labeled copolymers, Np-PEO-*block*-PMAA and Py-PEO-*block*-PMAA, are confined in close proximity within polymeric micelles, the interchromophore separation is within the range of NRET, and consequently, excitation at 290 nm will result in emissions from excited Np (λ : 310–400 nm) and from Py excited via NRET from Np* ($\lambda > 380$ nm). The effect is exemplified in Figure 3, where we present emission spectra of mixed solutions of Np-PEO-*block*-PMAA1 and Py-PEO-*block*-PMAA1 of pH 3.7 ($\alpha = 0$) and pH 6.7 ($\alpha = 0.62$) upon excitation at 290 nm. The total copolymer concentration (0.1 g/L) and the relative amounts of both copolymers are the same in the two solutions. Both spectra exhibit a contribution from Np* (300–360 nm) and a contribution from Py* (360–450 nm), but the emission originating from Py excited by NRET from Np* is much stronger, relative to the Np emission, in the solution of pH 3.7 than in the solution of pH 6.7. Emission spectra of solutions of Np-PEO-

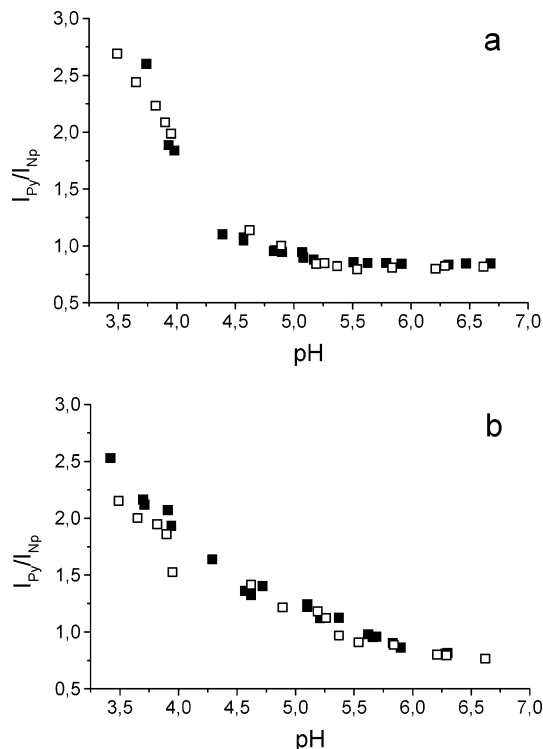


Figure 4. Changes in the ratio I_{Py}/I_{Np} of pyrene and naphthalene emission intensities as a function of pH for (a) PEO-*block*-PMAA1 and (b) PEO-*block*-PMAA2 solutions prepared by codissolution of dry samples (full symbols) or by mixing of preformed solutions (open symbols); polymer concentration = 0.1 g/L, $I = 10$ mM, $[Np]/[Py] = 4$.

block-PMAA1 of pH 3.7 and 6.5 are presented in Figure 3 as well to show the absence of Np excimer both at complexed and at uncomplexed state. This excludes the possibility that changes in Np monomer/excimer intensity ratio would interfere the NRET data. All spectra in Figure 3 are normalized to Np intensity.

A qualitative measure of the relative extent of energy transfer can be obtained by taking the ratio I_{Py}/I_{Np} of the intensity of the emission at 396 nm to that of the average of the emission intensities at 323 and 338 nm. In this scale, a larger value reflects a higher NRET efficiency. In our experiments, the largest value ($I_{Py}/I_{Np} = 2.7$) was recorded for mixed aqueous solutions of the fully protonated copolymers. It was much lower for mixed solutions of the ionized copolymers ($I_{Py}/I_{Np} = 0.8$). Having ascertained that NRET permits the detection of interpolymeric micelles and their disruption, we carried out sets of experiment allowing us to monitor closely the effect of α on the micellization of PEO-*block*-PMAA. Mixed solutions of the labeled copolymers were prepared either by mixing two preformed solutions of Np- and Py-labeled copolymers (neutral pH) or by codissolution of the Np- and Py-labeled copolymers into water and subsequent adjustment of the pH of the mixed solution. Emission of both sets of mixed solutions was measured for low to neutral pH in order to monitor the dependence of I_{Py}/I_{Np} on α . The trends are depicted in Figure 4, where we plot I_{Py}/I_{Np} as a function of pH for mixed solutions of PEO-*block*-PMAA1 (a) and PEO-*block*-PMAA2 (b) in relative amounts such that $[Np]/[Py] = 4$. Focusing first on Figure 4a, we note a sharp decrease, within a narrow range of pH (3.5–4.5), in I_{Py}/I_{Np} for the emissions of mixed solutions of the shorter block copolymer signaling a decline in NRET efficiency

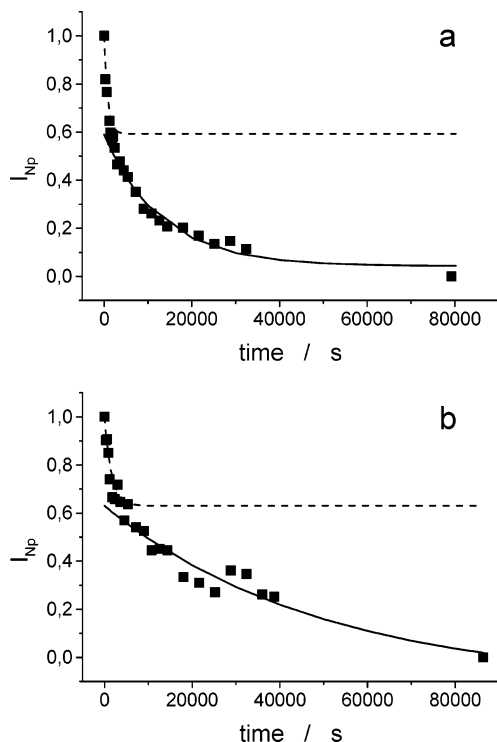


Figure 5. Changes in normalized naphthalene emission $I_{Np, norm}$ as a function of the time following the injection of a solution of Py-labeled copolymer to a solution of Np-labeled copolymer for (a) PEO-*block*-PMAA1 and (b) PEO-*block*-PMAA2 at pH 3.8. Data points were fitted to the insertion/expulsion model (dashed line) and the merging/splitting model (solid line).

and, consequently, the disruption of the polymer micelles. In mixed solutions of the longer block copolymer (PEO-*block*-PMAA2), the NRET efficiency also decreases with increasing α , but the changes occur over a wider range, an indication of some level of interpolymeric association, even under ionization conditions for which it was not possible to detect polymeric micelles by DLS (Figure 2). As described in the Experimental Section, mixed solutions were prepared either from predissolved copolymers or by codissolution of the copolymers. The efficiency of NRET was not affected by the preparation method, an indication that an equilibrium situation was established before the measurements (12 h).

To ascertain that equilibrium had indeed been reached, we monitored the decrease in Np emission intensity as a function of the time following injection of a Py-PEO-*block*-PMAA solution (pH 3.8, $\alpha = 0.01$) into a solution of Np-PEO-*block*-PMAA (pH 3.8, $\alpha = 0.01$) (Figure 5). Data were normalized to permit comparison of the chain exchange mechanism in solutions of the short and long copolymers and fitted to eq 2. The naphthalene emission intensity decreased promptly upon addition of Py-labeled copolymer, diminishing by nearly half its initial value within 1 h. However, it took ~ 14 h until no significant changes in I_{Py}/I_{Np} took place. The data presented in Figure 5 contain information on the actual mechanism of chain exchange, as described in the Discussion section.

Steady-State and Time-Resolved Fluorescence of Pyrene-Labeled Block Copolymers. To gain further insight into the pH dependence of the composition and fate of PEO-*block*-PMAA micelles, the photophysics of Py bound to the MAA blocks were scrutinized in the

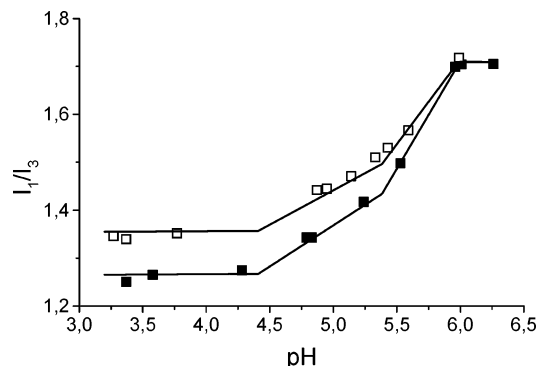


Figure 6. Changes in the ratio I_1/I_3 of pyrene emission intensities at 375 nm (I_1) and 386 nm (I_3) as a function of pH for solutions of Py-PEO-*block*-PMAA1 (solid symbols) and Py-PEO-*block*-PMAA2 (open symbols); polymer concentration = 0.1 g/L, $I = 10$ mM.

absence of Np-labeled copolymers. The steady-state fluorescence spectrum of Py-PEO-*block*-PMAA consists of an emission from spatially isolated pyrenes ("monomer emission") with the (0,0) band at 376 nm without any contribution from pyrene excimers, which can form if two Py are in close proximity. The low level of labeling accounts for the absence of excimer emission, often observed in aqueous solutions of Py-labeled water-soluble polymers.³² From the emission spectrum, we recorded as a function of pH the value of the ratio I_1/I_3 of the intensity of the (0,0) band, I_1 , to that of the (0,3) band, I_3 . The ratio gives an indication of the micropolarity sensed by the probe, increasing as the micropolarity experienced by the probe increases.³³ The emission spectra of derivatized pyrenes may lack the micropolarity sensitivity. Examples of such C-1 derivatives (as the one used in the present study) however exist that show environmental sensitivity, but the quantitative values of I_1/I_3 may differ to some extent in comparison to pyrene. Nevertheless, the qualitative information given by the I_1/I_3 ratio remains unchanged.^{32,34}

For solutions of either the short or the long block copolymer the I_1/I_3 ratio took a value of ~ 1.3 in solutions of the fully protonated copolymers ($\alpha = 0$), increasing slightly within $4.5 < \text{pH} < 5.5$ with increasing α up to a value of ~ 1.4 . A marked change in the ratio I_1/I_3 was observed in solutions of $\text{pH} > 5.5$: it rose sharply in a narrow range of pH to reach a maximum value of ~ 1.7 , a value close to the typical one of pyrene in a polar environment. The changes in I_1/I_3 with pH for solutions of each labeled copolymer are presented in Figure 6. We note that for all pH values the microenvironment experienced by Py is slightly less polar in solutions of Py-PEO-*block*-PMAA1, which possesses a shorter MAA block compared to Py-PEO-*block*-PMAA2. In consequence, a greater fragment of the pyrene labels is located in the hydrophobic core of the particles in the case of the shorter PEO-*block*-PMAA1. The data recorded for solutions of the block copolymers (Figure 6) also allow the detection of the breaking of the intramolecular hydrogen bonding as well as the full extension of the PMAA chain but seem rather insensitive to the disruption of the polymeric micelles, which takes place in solutions of lower pH and was observed by DLS and NRET experiments.

Further information on the polymeric micelle micropolarity and pH-triggered disruption was gathered from time-resolved fluorescence measurements, based on the

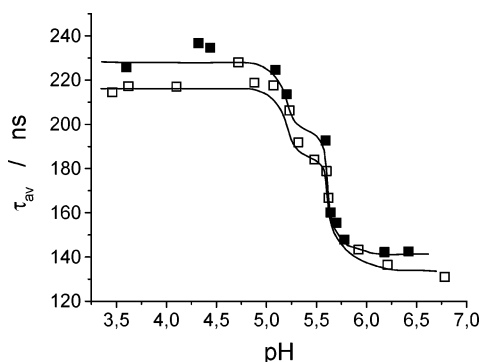


Figure 7. Changes on the average lifetimes, τ_{av} , of pyrene for solutions of Py-PEO-*block*-PMAA1 (solid symbols) and Py-PEO-*block*-PMAA2 (open symbols) as a function of pH; polymer concentration = 0.1 g/L, $I = 10$ mM.

fact that the fluorescence lifetime of pyrene is longer in apolar media.³⁴ The fluorescence lifetime of pyrene in the fully protonated copolymers Py-PEO-*block*-PMAA1 and Py-PEO-*block*-PMAA2 consisted of two components: a long-lived component (250 ns, 80% of the total intensity) and a short-lived component (70 ns). Both the lifetime and the fraction of the long-lived component exhibit a remarkable dependence on the degree of ionization of the copolymer. The long lifetime is constant in solutions of $\text{pH} < 5.0$ ($\alpha < 0.16$); it decreases rapidly with increasing ionization, reaching a plateau value of ~ 170 ns for $\text{pH} = 5.5$ ($\alpha = 0.3$) and undergoes a second decrease to a value of 140 ns as pH reaches 6.0 ($\alpha = 0.42$). The contribution to the total Py lifetime of the long-lived component remains constant up to $\text{pH} 5.5$ ($\alpha = 0.3$), but it exceeds 95% in the fully ionized copolymers. In contrast, the contribution and lifetime of the short-lived component are not affected as the solution pH is increased until the pH reaches a value of ~ 5.5 ($\alpha = 0.3$). Its contribution then diminishes with further increase in pH value. The presence of two lifetime components is taken as an indication of the presence of two populations of pyrene labels that experience different environments. In solutions of neutral polymeric micelles, the long-lived component corresponds to Py labels in the nonpolar micellar core environment, while the short-lived component originates from Py labels experiencing the polar environment of the micelle corona. In solutions of high α , all of the pyrene labels experience the same polar environment, as isolated copolymer chains take up their fully expanded conformation. The time dependent data are represented in Figure 7, where we plot the changes in the average Py lifetime as a function of the pH of the solutions. The curves for both copolymers present two transitions: one for $\text{pH} 5\text{--}5.5$, which, from I_1/I_3 measurements, we can assign to the disappearance of the hydrogen bonds between MAA and EO units, and a second transition for $\text{pH} 5.5\text{--}6.0$, ascribed to the full extension of the ionized copolymer. Fluorescence studies using either pyrene probe added to solutions of PMAA or pyrene linked to PMAA have shown a corresponding sharp change in the emission intensity of Py, which was taken as an indication of the transition from the coiled conformation of partially ionized PMAA to the extended conformation taken by the fully ionized PMAA.³⁵ In these studies it was noted that, whereas Py dissolved as a probe in PMAA solutions was released in the polar aqueous environment in solutions of $\text{pH} \sim 5$, Py linked to the polymer chain remained protected from the aqueous environment until the solution pH reached the

value 5.5 characteristic of the conformation change corresponding to the release of inter-methyl hydrophobic interactions.

Discussion

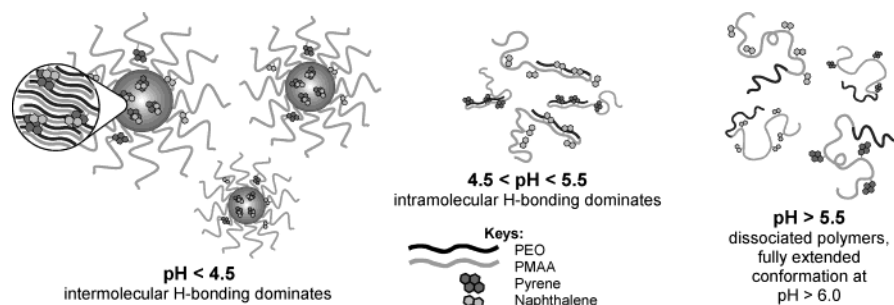
According to the data presented above, four main phases can be recognized from the different conformational states and types of interactions, which are depicted in Scheme 1. Within phase I, $\text{pH} < 4.5$, $\alpha < 0.07$, the hydrophobicity of the H-bonded complexed segments exceeds the capability of the uncomplexed PMAA segments to keep the polymers dissolved on a molecular level, and therefore intermolecular self-complex particles are formed. Within this pH range, the polarity of the Py environment remains unchanged as is observed from the I_1/I_3 and the lifetime data. However, the extent of NRET decreases as pH increases, which is indicative of reducing compactness of the particles. The distance between the chain segments increases in the particle core, and subsequently Py and Np labels are pulled further apart. Also, it appears that the stabilizing power of the PMAA segments increases even due to a minor increase in the degree of ionization of the carboxylic groups, and consequently, fewer polymers are driven together and the particle size decreases slightly. Further ionization of the acid groups destabilizes the intermolecular particles, and they break apart as seen from the disappearance of NRET and the strong reduction of the particle size. Within phase II, $4.5 < \text{pH} < 5.5$, $0.07 < \alpha < 0.3$, the intrapolymeric H-bonding dominates. The block copolymers are unimolecularly dissolved but still contracted as seen from the smaller particle size when compared to higher pH solutions. Also, the surroundings that the Py labels experience are less polar than aqueous environment. Above $\text{pH} 5.5$ (phase III, $0.3 < \alpha < 0.42$) also the intrapolymeric H bonds have broken up, and the polymers have adopted an uncomplexed coil conformation. The fully extended coil conformation is achieved however only at $\text{pH} 6$ (phase IV, $\alpha > 0.42$) when the contracting effect of the hydrophobic methyl groups of the MAA units is correlated by the increased degree of ionization.

Critical pH Values. Depending on the analysis method, different characteristic degrees of ionization or pH values for complexation of PEO and PMAA have been observed. Poe et al.¹⁴ studied a system consisting of PEO grafted PMAA, PMAA-*graft*-PEO, in comparison to the homo-PMAA and a mixture of PEO and PMAA homopolymers with NMR and DLS. By NMR, the T_2 relaxation of protons of EO units was measured vs solution pH as well as the polymer self-diffusion by pulsed gradient spin-echo (PGSE) experiments. They went through a pH range 5–10.5. Congruent to our findings, the intrapolymeric H-bonding was observed to occur at $\text{pH} < 5.6\text{--}5.7$, corresponding $\alpha = 0.3\text{--}0.35$. The reference mixture of homopolymers did not, however, show any signs of H-bonding down to $\text{pH} 5$ ($\alpha = 0.15$). Any intermolecular interactions were not observed by either the PGSE or the DLS experiments in the polymer systems within the studied pH range.

Gohy et al.¹⁷ studied the complexation of PEO-*block*-PMAA copolymers where the EO units were in substantial excess ($X_{n,\text{PEO}} = 177$ and $X_{n,\text{PMAA}} = 21$) by DLS. In contrast to the present study and Poe et al.,¹⁴ the formation of interpolymeric particles was seen to take place at $\text{pH} \leq 5.5$, corresponding to $\alpha = 0.3$.

A study by Podhájecká et al.³⁶ serves an extreme example of the complexation of PEO and PMAA in

Scheme 1



aqueous solution of elevated pH. They studied hybrid polymeric micelles with compact polystyrene cores (PS) and mixed PMAA/PEO shells, where the $M_{w,PMAA} > M_{w,PEO}$, by light scattering, fluorescence spectroscopy and potentiometric measurements. They found that the interpolymer PMAA/PEO complex in the inner part of the shell is very stable toward changes in the bulk conditions. Even at strongly alkaline solutions, the carboxylic groups of the innermost part of PMAA shell are never dissociated, and the H bonds between MAA and EO units remain intact. The influence of the frozen nature of the PS core, as well as the low polarity of the inner shell it induces, is emphasized for understanding such behavior of the mixed shells.

Frank et al.^{11,12} have studied a mixed system of PEO and PMAA or PAA homopolymers by fluorescence spectroscopy where PEO was labeled from both ends by Py fluorophores. They found that there was complexation between PEO and PMAA when the degree of ionization of the PMAA was less than 0.3. However, at this α PMAA has adopted the compressed coil conformation due to the methyl group of MAA unit, thereupon offering a more favorable hydrophobic surrounding environment for the Py labels in the PEO chain ends in comparison to the aqueous media. Similar abrupt coil compression does not occur in the case of PAA, and therefore the PEO–PAA complexes are less stable. The complexation of PEO–PAA homopolymer mixture has been shown to occur only at $\alpha < 0.15$.^{37,38} Since the block copolymers of the present study are labeled on the PMAA block, the hydrophobic interactions cannot draw prematurely the PMAA and PEO blocks together. Therefore, the results of Frank et al. cannot be directly compared to the present study.

Zeghal et al.⁴ investigated the complexation of PMAA and PEO by small-angle neutron scattering (SANS). According to their results, as $\alpha > 0.1$ no complexation occurs, and the conformation of each polymer in the mixture resembles that of the same polymer alone in the solution at the same concentration.

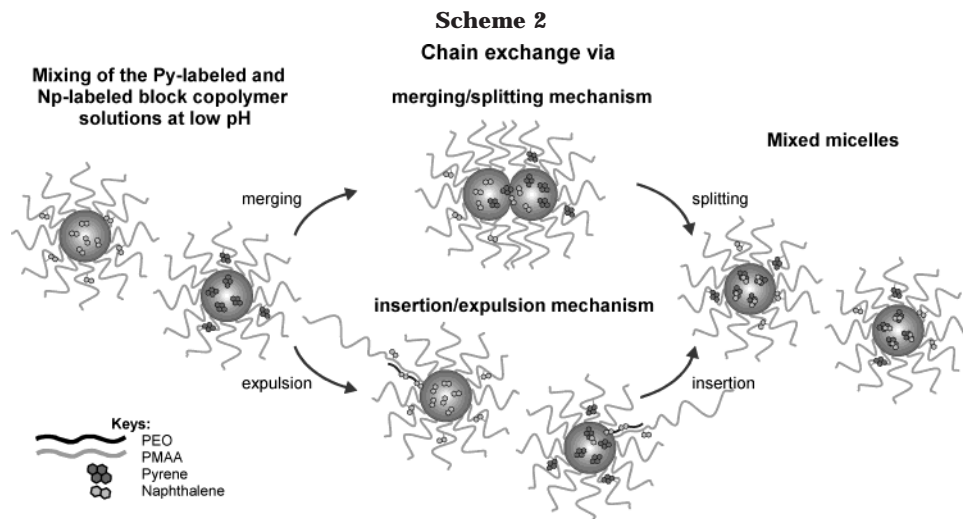
As concluded by Poe et al.¹⁴ for the graft copolymers, the covalent binding between the two polymers enhances the formation of H bonding in comparison to the mixtures of homopolymers, and the same conclusion may be drawn from the present study. The covalent binding of the PEO and PMAA blocks causes the intramolecular hydrogen bonding to take place at higher degree of ionization compared to the mixture of homopolymers. This finding is consistent with those of Klier et al.¹⁵ and Scranton et al.¹⁶ that the graft copolymers of PMAA and PEO form complexes under wider range of molecular weights and concentrations than mixtures of homopolymers. The difference in the complexation ability between the copolymers and mixture of homopolymers may be attributed to the net

complexation free energy. The loss in translational degrees of freedom is less in the case of copolymers than in the mixtures of homopolymers, and therefore the energy change becomes more favorable and the complexation takes place at wider range of molecular weights and concentrations as well as degrees of ionization.

Effect of the PMAA Block Length. In general, the behavior of the block copolymers with different PMAA block lengths is similar. The transitions between the different phases take place at same pH independent of the size of the block copolymer. Also, a different proportional amount of EO units does not affect the dissociation of PMAA block as indicated by the coinciding potentiometric titration curves (Figure 1). Similar potentiometric results were obtained by Poe et al. for PMAA-*graft*-PEG copolymers.¹⁴ The pK_a values of the graft copolymers deviated from those of a homo-PMAA at low α but coincided between graft copolymers with different PEG graft densities.

Some differences can, however, be observed in the solutions of the block copolymers with different PMAA block lengths. There is a difference in the polarity of the environment of the pyrene labels at low pH. The I_1/I_3 ratio of the shorter Py-PEO-*block*-PMAA1 is lower at low pH than in the case of the longer Py-PEO-*block*-PMAA2 (Figure 6). Also, at low pH the average lifetimes of the labels in Py-PEO-*block*-PMAA1 are somewhat longer in comparison to the labels in Py-PEO-*block*-PMAA2 (Figure 7). In both of the block copolymers the number of the MAA units is higher than the number of ethylene oxide units. It is the excess PMAA segments which then act as electrosteric stabilizers of the self-complex particles. Consequently, a greater fragment of the pyrene labels is located in the hydrophobic core of the particles in the case of the shorter PEO-*block*-PMAA1. The reason for the more extensive NRET in the particles of the shorter block copolymers is also the greater fragment of the buried fluorescence labels, though the molar ratio $[Np]/[Py] = 4$ was same in both experiments.

Though the excess MAA units stabilize the self-complex particles at low pH, the PEO blocks affect the solubility of the block copolymers at higher pH solutions. In the case of the shorter PEO-*block*-PMAA1, interpolymeric interactions are clearly present only at pH < 4.5. Whereas in the case of the longer PEO-*block*-PMAA2, the dissolving effect of the PEO block is not enough to prevent the presence of some interpolymeric interactions at pH < 5.5, which is the limiting pH for intramolecular H bonding. Apparently, the NRET rises from some temporal aggregates or “slow collisions” between two block copolymers at $4.5 < \text{pH} < 5.5$, since the DLS data do not show any signs of bigger particles. The NRET experiments of both of the block copolymers are however



independent of the method of sample preparation. Therefore, the effect of the hydrophobic nature of the fluorescence labels on the block copolymers behavior in aqueous solutions can be excluded.

Chain Exchange between Self-Complex Particles. The chain exchange reactions between micelles composed of small molecular surfactants occurs fast and the mechanism of the exchange is the insertion and expulsion of the unimers.^{39,40} The earliest kinetic studies on the chain exchange between polymer complexes were done with complexes of the homopolymers of ethylene oxide, acrylic acid, and vinylpyrrolidone.^{13,41} Those studies as well as the more recent ones about the micelles composed of amphiphilic block copolymers have shown that the chain exchange occurs more slowly due to the more complicated diffusion of the polymeric segments.^{42–51} In addition, very often the exchange rate cannot be fitted single exponentially, independent of the polydispersity of the polymers.^{13,41,44–47} There are two basic mechanisms that are considered to give rise to chain exchange, insertion and expulsion of single chains, and merging and splitting of the micelles. A few theoretical studies have been performed about the chain exchange between polymeric micelles.^{52–54} The results have been contradictory to some extent. Halperin and Alexander⁵² concluded that the single chain insertion/expulsion is the only mechanism of the chain exchange, although the association/dissociation rates for micellar merging/splitting mechanism were not calculated. In the study of Dormidontova⁵⁴ the chain exchange mechanism was evaluated for a developing micelle system, and in the study by Haliloglu et al.⁵³ a micellar system in equilibrium was considered. Both studies emphasize the importance of both single chain insertion/expulsion and micellar merging/splitting mechanisms on the chain exchange dynamics.

In the present study, the stability of the self-complex particles toward chain exchange between particles was studied by means of NRET. The generally assumed chain exchange mechanisms are illustrated in Scheme 2. The experiments were conducted by mixing the low pH solutions of the naphthalene-labeled polymers and pyrene-labeled polymers. Subsequently, the decrease of the naphthalene intensity in the emission spectrum was monitored. The normalized intensity data were analyzed by using eq 2. Figure 5 presents the progress of the chain exchange between the particles as $I_{\text{Np, norm}}$ as well as the calculated curves for both the fast and slow fractions. Table 2 shows the kinetic coefficients.

Table 2. Kinetic Coefficients for Chain Exchange between the Self-Complexes at Low pH^a

	$k_1 \times 10^4$ (s ⁻¹)	f_1	$k_2 \times 10^4$ (s ⁻¹)	f_2	$k_{\text{av}} \times 10^4$ (s ⁻¹)
PEO- <i>block</i> -PMAA1	12.1	0.43	0.77	0.57	5.62
PEO- <i>block</i> -PMAA2	6.26	0.33	0.20	0.67	2.22

^a Determined from the decay of naphthalene intensity.

Both chain exchange mechanisms, insertion/expulsion of single chains and merging/splitting of the micelles, are nearly equally present in the chain exchange processes of the two block copolymers, PEO-*block*-PMAA1 and PEO-*block*-PMAA2. The merging/splitting of the micelles is the main mechanism and dominates clearly especially in the case of the longer PEO-*block*-PMAA2.

The length of the PEO block in both of the block copolymers is the same, $X_n = 113$, whereas the size of the PMAA block is different, $X_n = 122$ and $X_n = 294$ for PEO-*block*-PMAA1 and PEO-*block*-PMAA2, respectively. Consequently, the length of the core forming hydrogen-bonded segment can be considered to be equal in both cases. The size of the micelle may however be different due to the difference in the coronal stabilizing segment. The increasing core size slows down the chain diffusion.^{46,54} However, as the size of the micelles formed by the shorter block copolymers could not be determined (PEO-*block*-PMAA1 precipitates at low pH at concentrations required for DLS), it is not possible to say how much the size of the core affects the rate of diffusion of the insoluble segment. The thickness of the corona varies significantly. The micelles consisting of the shorter PEO-*block*-PMAA1 have a very thin corona in comparison to the micelles consisting of the longer PEO-*block*-PMAA2, which have a thick corona. Very often it is the diffusion of the single chain through the corona or the deformation of the corona prior to the micellar merging that is the rate-determining step in the chain exchange between micelles. Thus, the thickness of the corona has a remarkable influence on the chain exchange rate.^{46,54} As a result, kinetic coefficients for both events, insertion/expulsion and merging/splitting, are higher for the shorter block copolymer, PEO-*block*-PMAA1.

The molecular weights of the PMAA blocks also affect the mechanism of chain exchange. In the present case neither of the blocks is insoluble as such, but the core is formed due to the interactions between the two blocks.

Therefore, the compactness of the cores depends most probably on the length of the PMAA block. In the case of the longer PEO-*block*-PMAA2 in comparison to the shorter PEO-*block*-PMAA1, the structure of the cores may be less perfect and thus, less compact, due to the possibility of loop formation in the aggregates. This leads to a less sharp interface between the core and corona. In the study of Haliloglu et al.,⁵³ the effect of the interaction parameter, ϵ , on the chain exchange mechanism was examined. The interaction parameter simulates the quality of solvent for the insoluble block; the smaller the interaction parameter, the better the solvent. Consequently, smaller ϵ value leads to less compact core and to a dynamically active, fuzzy interface, in which many chains continually make unsuccessful attempts to escape the core, and only a few succeed in escaping as free chains. Thus, it is the collision of the two micelles with dynamically active interfaces that are responsible for the chain exchange via merging/splitting mechanism. The present experiments correspond to a system described above. Accordingly, because the particles composed of PEO-*block*-PMAA2 have less compact cores and fuzzier interface, the merging/splitting mechanism is even more important than in the case of the shorter PEO-*block*-PMAA1.

Conclusions

The self-complexation of PEO-*block*-PMAA block copolymers under varying pH has been studied by fluorescence spectroscopy and by dynamic light scattering. The covalent binding between the two polymers has been observed to enhance the formation of H bonding in comparison to the mixtures of homopolymers. In the case of the block copolymers the H bond formation takes place at pH < 5.5, corresponding to $\alpha < 0.3$, whereas in the mixed solutions of homopolymers H-bonds form only at $\alpha < 0.1$.

The self-complexation of PEO-*block*-PMAA copolymers can roughly be divided into regimes where the interactions are either intermolecular, pH < 4.5, i.e., $\alpha < 0.07$, or intramolecular, $\alpha > 0.07$. In more detailed categorization four different conformation regimes have been recognized. Within stage I, $\alpha = 0$ –0.07, the block copolymers form intermolecular aggregates. Within stage II, $\alpha = 0.07$ –0.3 (pH 4.5–5.5), the conformation of the block copolymers is governed by the intramolecular hydrogen bonding. Within stage III, $\alpha = 0.3$ –0.42 (pH 5.5–6), the polymer coils are still contracted due to the hydrophobic effect of methyl groups. Finally, in stage IV, $\alpha > 0.42$ (pH > 6), the block copolymers are in an open coil conformation typical for polyelectrolytes.

The NRET experiments are in accordance with the assumption that there are two mechanisms responsible for the chain exchange between the self-complex particles ($\alpha = 0$), namely, insertion/expulsion of single chains and merging/splitting of the self-complex particles. Independent of the molecular weight of the block copolymers, the merging/splitting is the dominant mechanism. The molecular weight affects, however, in a way that the slower merging/splitting mechanism is even more favorable in the case of the higher molecular weight PEO-*block*-PMAA2.

References and Notes

- (1) Israelachvili, J. N. *Intermolecular and Surface Forces*; Academic Press: London, 1992.
- (2) Oyama, H. T.; Tang, W. T.; Frank, C. W. *Macromolecules* **1987**, *20*, 1839–1847.
- (3) Iliopoulos, I.; Audebert, R. *Eur. Polym. J.* **1988**, *24*, 171–175.
- (4) Zeghal, M.; Auvray, L. *Europhys. Lett.* **1999**, *45*, 482–487.
- (5) Saito, S. *Colloid Polym. Sci.* **1979**, *257*, 266–272.
- (6) Ikawa, T.; Abe, K.; Honda, K.; Tsuchida, E. *J. Polym. Sci., Polym. Chem. Ed.* **1975**, *13*, 1505–1514.
- (7) Baranovsky, V.; Shenkov, S.; Rashkov, I.; Borisov, G. *Eur. Polym. J.* **1991**, *27*, 643–647.
- (8) Papisov, I. M.; Baranovskii, V. Y.; Kabanov, V. A. *Vysokomol. Soyed.* **1975**, *17*, 2104–2111.
- (9) Tsuchida, E.; Abe, K. *Adv. Polym. Sci.* **1982**, *45*, 1–125.
- (10) Bekturov, E.; Bimendina, L. A. *Adv. Polym. Sci.* **1981**, *41*, 100–147.
- (11) Oyama, H. T.; Hemker, D. J.; Frank, C. W. *Macromolecules* **1989**, *22*, 1255–1260.
- (12) Hemker, D. J.; Garza, V.; Frank, C. W. *Macromolecules* **1990**, *23*, 4411–4418.
- (13) Chen, H.; Morawetz, H. *Eur. Polym. J.* **1983**, *19*, 923–928.
- (14) Poe, G.; Jarrett, W.; Scales, C.; McCormick, C. *Macromolecules* **2004**, *37*, 2603–2612.
- (15) Klier, J.; Scranton, A.; Peppas, N. *Macromolecules* **1990**, *23*, 4944–4949.
- (16) Scranton, A.; Klier, J.; Peppas, N. *J. Polym. Sci., Polym. Phys.* **1991**, *29*, 211–224.
- (17) Gohy, J.-F.; Varshney, S. K.; Jérôme, R. *Macromolecules* **2001**, *34*, 3361–3366.
- (18) Holappa, S.; Karesoja, M.; Shan, J.; Tenhu, H. *Macromolecules* **2002**, *35*, 4733–4738.
- (19) Holappa, S.; Andersson, T.; Kantonen, L.; Plattner, P.; Tenhu, H. *Polymer* **2003**, *44*, 7907–7916.
- (20) Mathur, A.; Drescher, B.; Scranton, A.; Klier, J. *Nature (London)* **1998**, *392*, 367–370.
- (21) Andersson, T.; Holappa, S.; Aseyev, V.; Tenhu, H. *J. Polym. Sci., Part A: Polym. Chem.* **2003**, *41*, 1904–1914.
- (22) Morawetz, H. *Macromolecules* **1996**, *29*, 2689–2690.
- (23) Katchalski, A. *J. Polym. Sci.* **1951**, *7*, 393–412.
- (24) Anghel, D. F.; Alderson, V.; Winnik, F. M.; Mizusaki, M.; Morishima, Y. *Polymer* **1998**, *39*, 3035–3044.
- (25) Wang, K. T.; Iliopoulos, I.; Audebert, R. *Polym. Bull. (Berlin)* **1988**, *20*, 577–582.
- (26) Nagasawa, M.; Murase, T.; Kondo, K. *J. Phys. Chem.* **1965**, *69*, 4005–4012.
- (27) Leyte, J. C.; Mandel, M. *J. Polym. Sci., Part A: Polym. Chem.* **1964**, *2*, 1879–1891.
- (28) Wang, C.; Ravi, P.; Tam, K. C.; Gan, L. H. *J. Phys. Chem. B* **2004**, *108*, 1621–1627.
- (29) Lakowitz, J. R. *Principles of Fluorescence Spectroscopy*, 2nd ed.; Kluwer Academic/Plenum Publishers: New York, 1999; Chapters 13–15.
- (30) Ringsdorf, H.; Simon, J.; Winnik, F. M. *Macromolecules* **1992**, *25*, 5353–5361.
- (31) Winnik, F. M. *Polymer* **1990**, *31*, 2125–2134.
- (32) Winnik, F. M.; Regismond, S. T. A. *Colloids Surf., A* **1996**, *118*, 1–39.
- (33) Kalyanasundaram, K.; Thomas, J. K. *J. Am. Chem. Soc.* **1977**, *99*, 2039–2044.
- (34) Morishima, Y.; Tominaga, Y.; Kamachi, M.; Okada, T.; Hirata, Y.; Mataga, N. *J. Phys. Chem.* **1991**, *95*, 6027–6034.
- (35) Chu, D.-Y.; Thomas, J. K. *Macromolecules* **1984**, *17*, 2142–2147.
- (36) Podhájecká, K.; Štěpánek, M.; Proháčka, K. *Langmuir* **2001**, *17*, 4245–4250.
- (37) Iliopoulos, I.; Audebert, R. *Polym. Bull. (Berlin)* **1985**, *13*, 171–178.
- (38) Iliopoulos, I.; Halary, J.; Audebert, R. *J. Polym. Sci., Polym. Chem. Ed.* **1988**, *26*, 275–284.
- (39) Aniansson, E. A. G.; Wall, S. N. *J. Phys. Chem.* **1974**, *78*, 1024–1030.
- (40) Aniansson, E. A. G.; Wall, S. N.; Almgren, M.; Hoffmann, H.; Kielmann, I.; Ulbricht, W.; Zana, R.; Lang, J.; Tondre, C. *J. Phys. Chem.* **1976**, *80*, 905–922.
- (41) Chen, H.; Morawetz, H. *Macromolecules* **1982**, *15*, 1445–1447.
- (42) Wang, Y.; Balaji, R.; Quirk, R. P.; Mattice, W. L. *Polym. Bull. (Berlin)* **1992**, *28*, 333–338.
- (43) Bednář, B.; Edwards, K.; Almgren, M.; Tormod, S.; Tuzar, Z. *Makromol. Chem., Rapid Commun.* **1988**, *9*, 785–790.
- (44) Wang, Y.; Kausch, C. M.; Chun, M.; Quirk, R. P.; Mattice, W. L. *Macromolecules* **1995**, *28*, 904–911.

- (45) Procházka, K.; Bednář, B.; Mukhtar, E.; Svoboda, P.; Trněná, J.; Almgren, M. *J. Phys. Chem.* **1991**, *95*, 4563–4568.
- (46) Tian, M.; Qin, A.; Ramireddy, C.; Webber, S. E.; Munk, P. *Langmuir* **1993**, *9*, 1741–1748.
- (47) Underhill, R. S.; Ding, J.; Birss, V. I.; Liu, G. *Macromolecules* **1997**, *30*, 8298–8303.
- (48) Creutz, S.; van Stam, J.; Antoun, S.; De Schryver, F. C.; Jérôme, R. *Macromolecules* **1997**, *30*, 4078–4083.
- (49) Creutz, S.; van Stam, J.; De Schryver, F. C.; Jérôme, R. *Macromolecules* **1998**, *31*, 681–689.
- (50) van Stam, J.; Creutz, S.; De Schryver, F. C.; Jérôme, R. *Macromolecules* **2000**, *33*, 6388–6395.
- (51) Smith, C. K.; Liu, G. *Macromolecules* **1996**, *29*, 2060–2067.
- (52) Halperin, A.; Alexander, S. *Macromolecules* **1989**, *22*, 2403–2412.
- (53) Haliloglu, T.; Bahar, I.; Erman, B.; Mattice, W. L. *Macromolecules* **1996**, *29*, 4764–4771.
- (54) Dormidontova, E. E. *Macromolecules* **1999**, *32*, 7630–7644.

MA049153N